Weeds-wheat discrimination using hyperspectral imagery

X. Hadoux, N. Gorretta, Gilles Rabatel

Weeds-wheat discrimination using hyperspectral imagery

Xavier Hadoux[1]*, Nathalie Gorretta[1], Gilles Rabatel[1]

[1]*Irstea UMR ITAP, 361 rue J-F Breton BP 5095, 34196 Montpellier Cedex 5, France*
**Corresponding author. E-mail: xavier.hadoux@irstea.fr*

Abstract

The difficulties to efficiently discriminate between weeds and crop by computer vision remains today a major obstacle to the promotion of localized weeding practices. The objective of the present study was to evaluate the potential of hyperspectral imagery for the detection of dicotyledonous weeds in durum wheat during weeding period (end of winter). An acquisition device based on a push-broom camera mounted on a motorized rail has been used to acquire top-view images of crop at a distance of one meter. A reference surface set in each image, as well as specific spectral pre-processing, allow overcoming variable outdoor lighting conditions. Spectral discrimination between weeds and crop, obtained by PLS-LDA, appears quite efficient, with a 8% prediction error on an independent test set.

Key words: hyperspectral imagery, classification, weed detection, PLS-LDA.

1. Introduction

Precision Agriculture concept relies on the spatial modulation of crop processing operations, for a better adaptation to heterogeneities inside the parcel. This concept, which was raised more than twenty years ago, is now currently applied in nitrogen input management, allowing a better control on yield and product saving.

However, for weeding operations, despite considerable environmental and economical issues, the common practice still consist in applying an assurance strategy: herbicides are uniformly spread over the entire parcel whatever is the actual level of infestation.

The reason is mainly technological. Currently some devices are proposed on the market to operate localized spraying of herbicides on bare soil (the vegetation being detected by photocells). However, no commercial setup addresses localized weeding operations after crop emergence, because it requires a perception system based on computer vision, able to discriminate weeds from crop.

Indeed, the identification of species inside vegetation is today the main obstacle to localized weeding. Numerous scientific studies have addressed this problem, and can be classified in two main approaches (Slaughter et al., 2008):

- The spectral approach, which focuses on the plant reflectance, and involves multispectral or hyperspectral imagery (Feyaerts & van Gool, 2001), (Vrindts et al., 2002). In this case, the difficulty consists in establishing spectral differences that are robust with respect to variable lighting conditions.

- The spatial approach, which relies on spatial criteria such as plant morphology (Chi et al., 2003), (Manh et al., 2001), texture analysis (Burks et al., 2000) or spatial organization (Gée et al., 2008). In this case, the natural complexity and variability of vegetation scenes are the main difficulties for classification.

The study presented here follows the first approach, in the particular case of durum wheat crop. The objective was to evaluate, as a first step, if the leaf reflectance contains enough spectral information to make a reliable discrimination between crop and dicotyledonous weeds. For this purpose, hyperspectral images of crop scenes have been acquired during the weeding period. Then specific correction procedures have been applied to overcome the variability of lighting conditions and of spatial orientation of leaves in natural crop scenes.

Finally, a Partial Least Square Linear Discrimination Analysis (PLS-LDA) discrimination model has been calibrated and tested on the corrected hyperspectral images. The discrimination results are presented and discussed.

2. Material and methods

2.1. Image acquisition and correction

Hyperspectral images of durum wheat have been acquired in an experimental station near Montpellier, south of France, in March 2011 and 2012. Images were acquired using a device specially developed by Irstea for in-field short-range hyperspectral imagery. The device consists in a push-broom CCD camera (HySpex VNIR 1600-160, Norsk Elektro Optikk, Norway) fitted on a tractor-mounted motorised rail. The camera has a spectral range from 0.4 µm to 1µm with a spectral resolution of 3.7nm. The first dimension of the CCD matrix is the spatial dimension (1600 pixels across track) and the second dimension is the spectral dimension (160 bands).

Each image represents about 0.30m across track by 1.50m along track seen at 1m above the canopy, the lens, and the view angle being fixed. The spatial resolution across track is 0.2 mm. The spatial resolution along track, depending on the motion speed, has therefore been adjusted.

In Fig. 1, two hyperspectral images are shown with false colours, i.e. using 3 bands respectively at 615, 564 and 459 nm as R, G, and B channels. These images illustrate the difference in lightning conditions we have to face in the following.

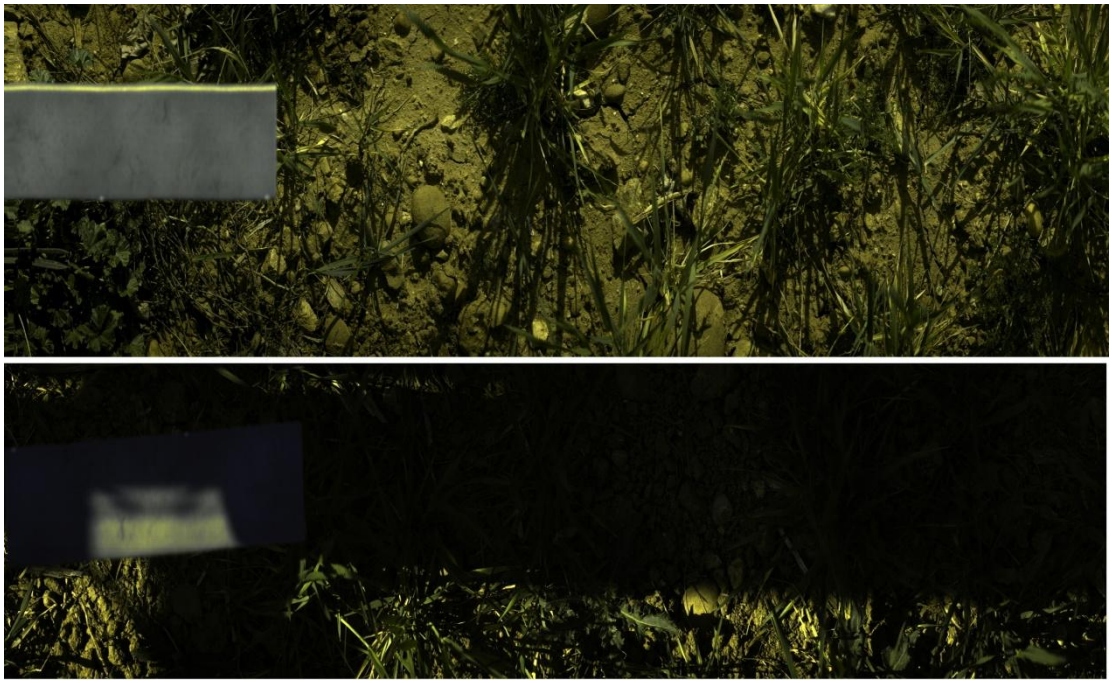

FIGURE 1: Two reflectance images in false RGB colours with different lighting conditions without shadow (up), with shadows (down). On the left : the ceramique plate.

In order to be able to compare spectral data collected in different outdoor conditions, it is necessary to have hyperspectral images independent of illumination, i.e. reflectance images. The reflectance of a given material is the ratio of reflected light to incident light. Therefore, we need to know solar lighting at each acquisition time. Hence, Spectralon™ (Labsphere, Inc., New Hampshire, USA.) is generally used because it is a lambertian surface and it

reflects 99 % of received signal whatever the wavelength. Therefore, it provides a good approximation of solar incident light in outdoor conditions. However, in our case, we have chosen to use a commercial ceramic plate, which is more robust to damage or dirt due to field experiment conditions.

The bidirectional reflectance distribution function (BRDF) of the ceramic has been measured in laboratory. As for many ordinary materials, it is the summation of a lambertian term and a specular term, the latter depending on the incident and viewing angles. However, because the specular term is directive enough, it can be totally neglected in our field operating conditions (horizontal plate observed with a zenithal view under non-zenithal solar lighting incidence, according to the latitude and season). We can thus consider the ceramic plate as a lambertian material with a known hemispheric reflectance $Rc(\lambda)$

Finally, for a given luminance image, the average luminance $Lc(\lambda)$ measured on the ceramic plate can be used to compute the horizontal irradiance $E(\lambda)$ on the scene $E(\lambda) = Lc(\lambda) / Rc(\lambda)$ .This allows applying the following reflectance correction to every pixel in the image:

$$R(x, y, \lambda) = L(x, y, \lambda) / E(\lambda) = \frac{L(x, y, \lambda).Rc(\lambda)}{Lc(\lambda)} \quad (1)$$

Where (x, y) are the pixel coordinates and λ the wavelength.

The reflectance correction specified in (1) takes into account the irradiance $E(\lambda)$ measured by means of a horizontal ceramic plate. However, leaf surfaces in the vegetation scene are not horizontal. Therefore, their irradiance can be higher or lower than the ceramic plate's one, according to the cosine of the angle between their surface normal and the lighting incidence. This introduces an unknown multiplicative factor k_1 on the pixel spectrum collected in the reflectance image, with respect to the real leaf reflectance.

Also, the BRDF of leaves includes a specular term (Bousquet et al., 2005). Due to a random spatial orientation, this specular reflection may be directed toward the image sensor. The corresponding specular light is not spectrally modified by the material and only contributes to the apparent reflectance as an additive term k_2.

As a summary, the leaf pixel values in the reflectance image do not correspond to the actual leaf lambertian reflectance $R_f(x, y, \lambda)$ but to an apparent reflectance:

$$R_{app} = R_f(x, y, \lambda) \cdot k_1 + k_2 \quad (2)$$

Where k_1 and k_2 are unknown terms.

In order to remove these unknown terms, a Standard Normal Variate (SNV) transformation will be applied consistently to all spectra before any further processing. It consists in centring the spectrum and setting its standard deviation equal to one.

2.2. Modelling procedure (experiment's design)

Since we have an important amount of spectra, we choose to build the model which gives the most reliable error estimation using an independant test set. In order to create this proper discrimination model, a calibration set, a validation set and a test set have to be built. A major sampling condition we took into consideration while designing the experiment is the independence between each set. For this purpose, we first split our images into three

groups. Then, in each of these groups, we have manually selected some spectra according to three classes: durum wheat, dicotyledonous weeds and soil. By this way, in each set, both X-values (spectrum) and Y-values (classes) are known. Y is coded using a disjunctive binary coding (0 or 1). Table 1 details the number of selected spectra in each class for each set.

TABLE 1: Experiment's design (number of spectrum samples per set)

	Calibration	Validation	Test
Wheat	200	200	320
Weed	150	150	240
Soil	150	150	240

In the following, the calibration set and the validation set are used only to create the classification model and to find the best number of Latent Variable (LV). The test set is used only to estimate the prediction error.

PLS-LDA

Because they contain accurate information about the chemical content of materials, spectra are often used for quantitative evaluation of component concentration, or for material discrimination. However, due to the high dimension of spectral data (hundreds of variables), classical multivariate regression or discrimination tools are not directly usable, and a first step of dimension reduction is generally required. In this context, the Partial-Least-Square (PLS) has become a very commonly used tool, thanks to its ability to determinate a pertinent subspace, called scores subspace, for a given regression problem. Unlike other dimension reduction methods, the PLS takes into account the covariance of both inputs and outputs to determine this scores subspace. To find the score subspace, PLS iteratively find the Latent Variables (LV) that produce the best trade-off between the explanation of the input, the explanation of the output, and the relation between the input and the output.

Then, both input and output are projected onto the formerly found LV and a new iteration begins. The number of iterations (the number of latent variables) is determined empirically using the V-shape of the Root Mean Square Error of Validation (RMSEV) described below.

Finally, a LDA is performed on the LV. This LDA consist in finding the linear subspace that allow the easiest discrimination. The well known solution to this problem is the subspace that maximise the variance between the classes and minimise the variance within the classes.

Calibration/Validation phase

During this phase, we want to figure out how many LV we need to keep for the model. To this purpose, we create a model using the variables in the calibration set. This procedure consists in creating models, with an increasing number of LV, using the calibration set. Applying these models on the validation set allows a computation of the RMSEV. The RMSEV is calculated by comparing the real $\mathrm{Y}_{\mathrm{val}}$ of the validation set with the estimated $\hat{\mathrm{Y}}_{\mathrm{val}}$ given by the model. Plotting this error for an increasing number of LV gives the commonly used V-shaped curve of RMSEV. The lowest RMSEV gives an estimation for the number of LV to keep. Another interesting plot present in Fig. 2 is the Root Mean Square Error of Calibration (RMSEC). This RMSEC is calculated by comparing $\mathrm{Y}_{\mathrm{cal}}$ and $\hat{\mathrm{Y}}_{\mathrm{cal}}$, where the latter represent the results testing the calibration model directly on the calibration data.

Test phase

Applying this model on the independent test set allows the calculation of the Root Mean Square Error of Prediction (RMSEP). This RMSEP is the most reliable measure of prediction for this kind of model.

3. Results and discussion

3.1. Model calibration/validation

In order to illustrate the classification procedure, the RMSEC and the RMSEV curves are plotted in Fig. 2, for 1 to 20 LV. According to this plot, 7 LV are chosen for the PLS-LDA model.

In Table 2 the resulting confusion matrix of the validation. As it could be expected, the best membership estimation is obtained for the soil, which is spectrally very different from vegetation. The classification performances are good, with a global error rate of 8.4% and a maximal error of 11%.

TABLE 2: Confusion matrix of validation

	Classified as wheat	Classified as weed	Classified as soil
Wheat	177 (88.5%)	22 (11%)	1 (0.5%)
Weed	16 (10.7%)	132 (88%)	2 (1.3%)
Soil	1 (0.6%)	0	149 (99.3%)

3.2. Model test

Then, applying this model onto the test set X_{test} and calculating the confusion matrix gives the results presented on Table 3. From these results, the global error of prediction is 7.9% which correspond to the global error during the validation. However, the maximal error is slightly superior with 14.6% of misclassified weed pixels.

TABLE 3: Confusion matrix of prediction

Classified as \ real	Classified as wheat	Classified as weed	Classified as soil
Wheat	293 (91.6%)	26 (8.1%)	1 (0.3%)
Weed	35 (14.6%)	205 (85.4%)	0
Soil	0	1 (0.4%)	239 (99.6%)

This test set validation confirms the robustness of the model created with a totally independent calibration test. Also, since images have been taken with a high difference of illumination, at different times and over two different years, we have a good chance that the model we produced will still be robust for the next season.

4. Conclusion

The results obtained above show the potential of detailed spectral information to discriminate vegetation species, provided the influence of lighting variability has been overcome using a reference material, and provided efficient chemometric tools such are PLS-LDA are utilised. However, despite the robustness, the classification errors are still important, due to the variability of the images taken at different time, different parcels and over two different years.

Moreover, the high number of required latent variables indicates that very tiny differences in the spectral shapes are taken into account to achieve an accurate discrimination.

The following step will be to evaluate the possibility of introducing spatial constraints to help the discrimination stage. Also, reducing the number of required bands, e.g. through a

detailed study of the latent variable shapes would open the door to an operational device based on multispectral image acquisition.

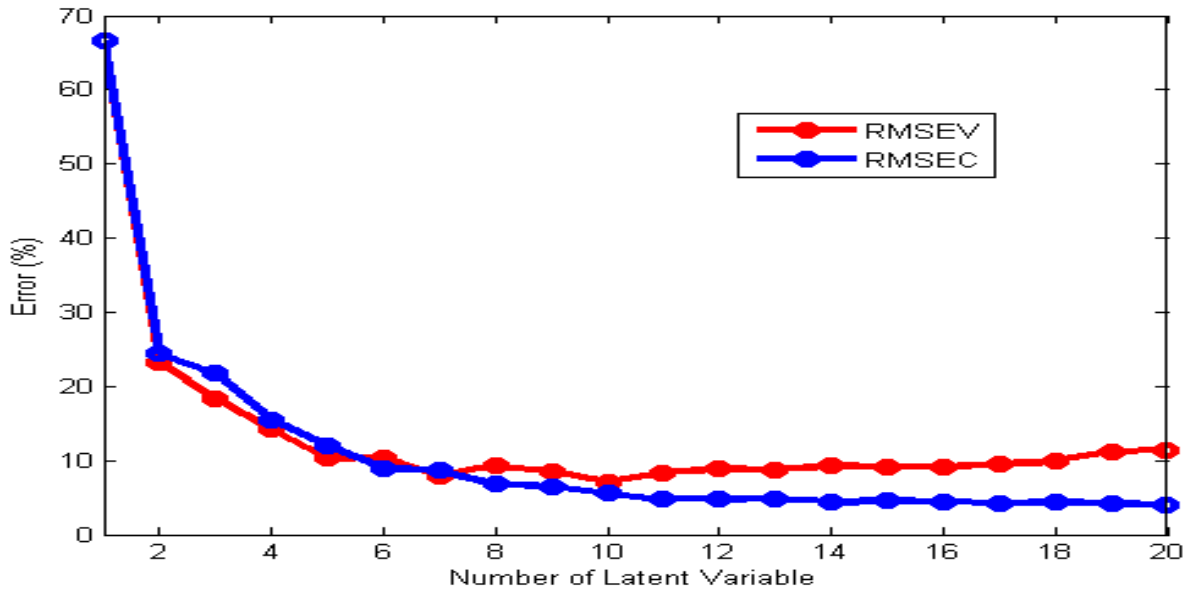

FIGURE 2: Red : Root Mean Square Error of Validation, Blue : Root Mean Square Error of Calibration, for 1 to 20 Latent Variables

Reference list

Bousquet L., S. Lachérade, S. Jacquemoud and I. Moya (2005). Leaf BRDF measurement and model for specular and diffuse component differentiation, Remote Sensing of Environment, 98(2-3), 201-211.

Burks, F.T, S.A. Shearer and F. A. Payne (2000). Classification of weed species using colour texture features and discriminant analysis. Transactions of the ASAE 43, 441-448.

Chi, T.Y, C.-F. Chien and T.-T. Lin (2003). Leaf shape modelling and analysis using geometric descriptors derived from Bezier curves. Transactions of the ASAE 46, 175-185.

Feyaerts, F. and L. van Gool (2001). Multi-spectral vision system for weed detection. Pattern Recognition Letters 22(6-7), 667-674.

Gée, C., J. Bossu, G. Jones and F. Truchetet (2008). Crop/weed discrimination in perspective agronomic images. Computers and Electronics in Agriculture 60(1), 49-59.

Manh, A.-G., G. Rabatel, L. Assemat, M.-J. Aldon (2001). Weed Leaf Image Segmentation by Deformable Templates. Journal of Agricultural Engineering Research 80(N°2), 139-146.

Slaughter, D.C., D.K. Giles and D. Downey (2008). Autonomous robotic weed control systems : A review. Computers and electronics in agriculture 61, 63 - 78

Vigneau, N., M. Ecarnot, G. Rabatel, P. Roumet (2011). Potential of field hyperspectral imaging as a non destructive method to assess leaf nitrogen content in Wheat. Field Crops Research 122(1), 25-31.

Vrindts, E., J. De Baerdemaeker and H. Ramon (2002). Weed Detection Using Canopy Reflection. Precision Agriculture 3(1), 63-80.